



Organic Acid Shift Reagents for the Discrimination of Carbohydrate Isobars by Ion Mobility-Mass Spectrometry

Journal:	<i>Analyst</i>
Manuscript ID	AN-ART-08-2020-001546.R1
Article Type:	Paper
Date Submitted by the Author:	03-Oct-2020
Complete List of Authors:	McKenna, Kristin; Georgia Institute of Technology College of Sciences, School of Chemistry and Biochemistry Li, Li; Georgia institute of Technology , School of Chemistry and Biochemistry Krishnamurthy, Ramanarayanan; TSRI, Chemsitry Liotta, Charles; Georgia Institute of Technology, Schools of Chemistry and Chemical Engineering Fernandez, Facundo; Georgia Institute of Technology, School of Chemistry and Biochemistry



Analyst

ARTICLE

Received 00th January 20xx,
Accepted 00th January 20xx
DOI: 10.1039/x0xx00000x

www.rsc.org/

Organic Acid Shift Reagents for the Discrimination of Carbohydrate Isobars by Ion Mobility-Mass Spectrometry.

Kristin R. McKenna^{ab}, Li Li^{abc}, Ramanarayanan Krishnamurthy^{ad}, Charles L. Liotta^{ab} and Facundo M. Fernández^{ab*}

Carbohydrates are the most abundant class of biomolecules on Earth with a diverse array of biological functions. It is hypothesized that they likely had an important role in the development of life on the primordial Earth as well. Since sugars have a variety of possible isobaric structures, it is necessary to characterize oligosaccharides beyond their molecular weight. Ion mobility-mass spectrometry (IM-MS) is a promising characterization technique for this purpose, as it is based on differences in charge and collision cross section (CCS). This study reports on the use of new noncovalent ligands as shift reagents to aid in the IM separations of disaccharides. A variety of organic acids were tested as shift reagents with traveling wave IM with the most promising ones being further investigated by drift tube IM. Drift tube IM provided higher resolution separations for the large majority of disaccharide complexes studied. Combining CCS results of the two most promising shift reagents allowed for the complete differentiation of all eight disaccharide standards examined in this study.

Introduction

Carbohydrates are vital to all forms of life, with significant roles in many biological processes that include signaling, metabolism, cellular recognition, protein post-translational modification, and growth regulation.¹⁻⁶ Sugars also aid in the co-solubility of other biomolecules due to their intermediate polarity, so it is likely that they may have also been important for the origins of life on the prebiotic Earth.⁷ Stern *et al.* and Tolstoguzov have each separately hypothesized that a carbohydrate world could have been the precursor to an RNA, DNA, and protein world based upon the properties and possible functions of saccharides.⁷⁻⁸ A prebiotically-plausible method to synthesize oligosaccharides has recently been reported by Li *et al.*, showing that, indeed, oligosaccharides could have been generated on the early Earth through dry-wet cycling reactions.⁹ Despite their importance, oligosaccharides are understudied compared to other biomolecules within the field of prebiotic chemistry.^{8, 10} This is partially because carbohydrate structures are complex to analyze, as they include different positional, structural, and stereoisomers. Unlike proteins and nucleic acids, oligosaccharides often

branch, leading to a higher level of structural diversity than for the other major classes of biopolymers.

Isomeric oligosaccharides can have vastly different functions, and it is therefore important to fully characterize their structures. Moreover, cross-linking with carbohydrates can cause large changes in properties of proteins, such as altering their stability or three-dimensional structure.¹¹ Reducing sugars, which have a free anomeric hydroxyl group and thus contain a hemiacetal, are more reactive and are consequently more likely to react with amino acids and other biomolecules.¹²⁻¹³ The protective role of oligosaccharides is generally associated with non-reducing species that do not have a free anomeric hydroxyl group and thereby, do not contain a hemiacetal group.¹⁴

Many analytical methods have been developed for oligosaccharide characterization. Liquid chromatography (LC), for example, has been extensively used for oligosaccharide separations, with its major advantages being high specificity for derivatized carbohydrates and the capability to perform quantitative analysis.¹⁵⁻¹⁷ LC can be used in conjunction with tandem mass spectrometry (MS/MS) to further increase specificity with similar or lower experiment times. MS/MS can also be used as a standalone technique to decrease the time required to analyze oligosaccharides, as MS/MS does not rely as heavily on derivatization and is much faster than LC. While MS/MS can efficiently distinguish relatively pure disaccharide samples, it can have limited success for the characterization of lower abundance components in complex mixtures of isobaric carbohydrates due to precursor ion co-selection, requiring additional information from another complementary technique such as nuclear magnetic resonance (NMR) spectroscopy or LC for full characterization of these complex mixtures.¹⁸⁻¹⁹

Ion mobility-mass spectrometry (IM-MS) has been established as a suitable complement to both LC and

^a NSF/NASA Center for Chemical Evolution

^b School of Chemistry and Biochemistry, Georgia Institute of Technology, Atlanta GA 30332, USA.

^c Current affiliation: Center for Alzheimer's and Neurodegenerative Diseases, Department of Biochemistry, University of Texas Southwestern Medical Center, Dallas, TX 75390.

^d Department of Chemistry, The Scripps Research Institute, 10550 North Torrey Pines Road, La Jolla, CA 92037 USA.

* E-mail: facundo.fernandez@chemistry.gatech.edu; Fax: +1 (404) 894-7452; Tel: +1 (404) 385-4432

Electronic Supplementary Information (ESI) available: [details of any supplementary information available should be included here]. See DOI: 10.1039/x0xx00000x

MS/MS.²⁰⁻²¹ IM-MS involves the separation of gas phase ions under an electric field while undergoing collisions with inert gas molecules on a millisecond time scale. The drift time (t_d) of an ion is related to its rotationally-averaged collision cross section (CCS), so IM can help to distinguish isobaric species. For example, IM has previously been used in a study by Clowers *et al.* to separate isobaric sodium adducts of N-acetylated disaccharide and trisaccharide alditols.²² In this study, three distinct IM features were identified for the seven disaccharide isomers, and all three trisaccharide isomers were able to be baseline separated. Additionally, in a study by Kyle *et al.*, IM was used in LC-IM-MS to separate isomeric lipids.²³ Smith *et al.* have shown the utility of IM for distinguishing protein conformers produced during unfolding.²⁴

Multiple platforms for IM-MS experiments have been reported, including drift tube IMS (DTIMS)²⁵ and traveling wave IMS (TWIMS).²⁶ DTIM involves the separation of ions under a constant weak electric field.²⁷ In this case, CCS can be linearly correlated with t_d via the Mason-Schamp equation.²⁷ In contrast, TWIM involves alternating phases of an RF voltage being applied to adjacent ring electrodes and a series of DC pulses that drive ions toward the MS detector.²⁶ Drift times measured in TWIMS require calibration in order to indirectly derive CCS values.²⁸⁻³⁰

IM is a popular emerging technique in the field of carbohydrate separations. A study by Williams *et al.*, for example, compared the characterization of sodiated *N*-glycans by DTIM and TWIM-MS with theoretical modelling to investigate the gas-phase properties and conformations of those glycans.³¹ Additionally, Morrison *et al.* utilized DTIM-MS/MS to partially resolve five tetrasaccharide isomers as their adducts with several metal cations.³² Disaccharide isomers are generally much more difficult to separate by IM due to their smaller differences in CCS.³³⁻³⁵ This creates the need to utilize shift reagents and high-resolution IM in order to successfully distinguish them. Shift reagents are ligands that can covalently or noncovalently modify analytes to amplify their gas-phase CCS differences. The mobility of the analyte is thus "shifted" to less crowded areas of the analytical space, preventing overlaps and interferences. Previously reported shift reagents for disaccharide IM separations include alkali³³ and alkaline earth metal cations,^{31, 34} 1-phenyl-3-methyl-5-pyrazolone,³⁶ and 3-carboxy-5-nitrophenylboronic acid.³⁷⁻³⁸ Amino acids have previously been shown to have some promise for complexing with monosaccharide isomers to improve separations by Gaye *et al.*³⁹ In this study, several new non-covalent amino and α -hydroxy acid shift reagents that included glutamic acid, tyrosine, L-malic acid, and N-methyl-D-aspartic acid (NMDA), were investigated for the TWIM and DTIM separation of eight disaccharides such as cellobiose, sucrose, and maltose, which are important energy storage molecules in biology.⁴⁰

Experimental

Reagents and Chemicals

Isomaltose, trehalose, and cellobiose were obtained from TCI (Philadelphia, PA). Maltose, lactose, lactulose, sucrose, NMDA, arginine, tyrosine, lactic acid, 2-hydroxyhexanoic acid, N-methyl-L-glutamic acid, citric acid, and N-methyl-DL-aspartic acid were purchased from Sigma Aldrich (St. Louis, MO).

Melibiose was obtained from Fluka. L-malic acid and L-tartaric acid were purchased from VWR (Radnor, PA).

Noncovalent modification of carbohydrates for TWIM-MS Analysis

Stock solutions (1 mM) of carbohydrate standards (cellobiose, isomaltose, lactose, lactulose, maltose, melibiose, sucrose, and trehalose) and shift reagents (L-malic acid, NMDA, tyrosine, lactic acid, 2-hydroxyhexanoic acid, tartaric acid, arginine, N-methyl-L-glutamic acid, N-methyl-DL-aspartic acid, and citric acid) were prepared in water. Five μ L of the 1 mM carbohydrate solution and 5 μ L of the 1 mM shift reagent solution were added to 990 μ L of unbuffered deionized water prior to analysis.

TWIM-MS analysis

Traveling wave arrival time distribution (ATD) measurements were performed using SYNAPT G2 and G2-S HDMS ion mobility-mass spectrometers (Waters Corp., Wilmslow, UK). All experiments used direct infusion electrospray ionization. Ion source settings for positive and negative ion mode were as follows, respectively: capillary voltage, 3.0/-2.5 kV; cone voltage, 40 V; source temperature, 80 °C; desolvation temperature, 100/150 °C; desolvation gas flow 500 L h⁻¹; cone gas flow, 0 L h⁻¹. The travelling wave velocity was 500 m sec⁻¹ with a wave height of 40 V. Nitrogen was used as the drift gas in all cases. ^{TWIM}CCS_{N₂} calibration in negative ion mode was performed with both polyalanine and polymalic acid according to the methods reported by Forsythe *et al.*²⁹ In positive ion mode, ^{TWIM}CCS_{N₂} calibration was performed using polyalanine as the sole calibrant, following CCS values reported by Bush *et al.*^{29, 41} Tandem MS experiments were performed without IM on the Synapt G2-S instrument with collision energies of 1 and 2 eV and LM resolution values of 15 and 9 for positive and negative ion modes, respectively. For negative ion mode MS/MS experiments, the concentration for both lactose and L-malic acid were 10 μ M. For positive ion mode MS/MS experiments, the concentration for lactose and NMDA acid were 5 and 50 μ M, respectively. These concentrations were determined empirically to produce signals for MS/MS with good signal-to-noise ratios. For breakdown curve MS/MS experiments, an equal concentration of 35 μ M of lactose and each respective shift reagent was used. The resulting sigmoidal curves were fit in Origin 8.5 to determine their inflection points.

Molecular dynamics calculations

The L-malic acid and NMDA complexes for each of the eight disaccharide standards were investigated by density functional theory calculations based on those reported by Zheng *et al.*⁴² Two-dimensional structures for each of the eight standards and the two shift reagents were obtained from Chempidder as .mol files.⁴³ The Chemaxon Marvin Suite was used to calculate the pK_a of each hydrogen on each molecule to determine the most likely shift reagent binding sites. Avogadro was utilized to convert the two-dimensional structures into three-dimensional structures, as well as combining the disaccharide and shift reagent into the same file.⁴⁴ Preliminary geometry optimization was performed in Avogadro, followed by further optimization in NWChem⁴⁵ at the B3LYP theory level⁴⁶ using the 6-31G(d) basis set.⁴⁷

Drift tube ion mobility experiments

An EXCELLIMS MA3100 drift tube ion mobility spectrometer was coupled with an Orbitrap mass spectrometer for DTIM measurements at atmospheric pressure, as described previously by Keelor *et al.*⁴⁸. The drift gas temperature was 100 °C for positive ion mode experiments and 90 °C for negative ion mode experiments. The electrospray ion source was operated at 2.3 kV and -2.2 kV in positive and negative ion modes, respectively. The maximum injection time for the Orbitrap was set to 1000 ms. The length of the drift tube was 10.55 cm, and electric fields in the 758–853 V cm⁻¹ range were used. Gating voltages of 60 V for gate 1, and 81 V for gate 2 were empirically optimized to maximize ion transmission without excessive ion gate leakage. The drift gas was infused at 2.00 L min⁻¹ and removed at 0.50 L min⁻¹ to keep the system at atmospheric pressure (~740 Torr in Atlanta, GA, USA). The EXCELLIMS software program Vislon was used in “scan mode” to pulse the gates for 200 μs, with a delay of 20 ms between gates. Results were manually extracted from the Orbitrap software Xcalibur to Excel, and then processed in Origin 8.5.

Results and Discussion

Noncovalent modification

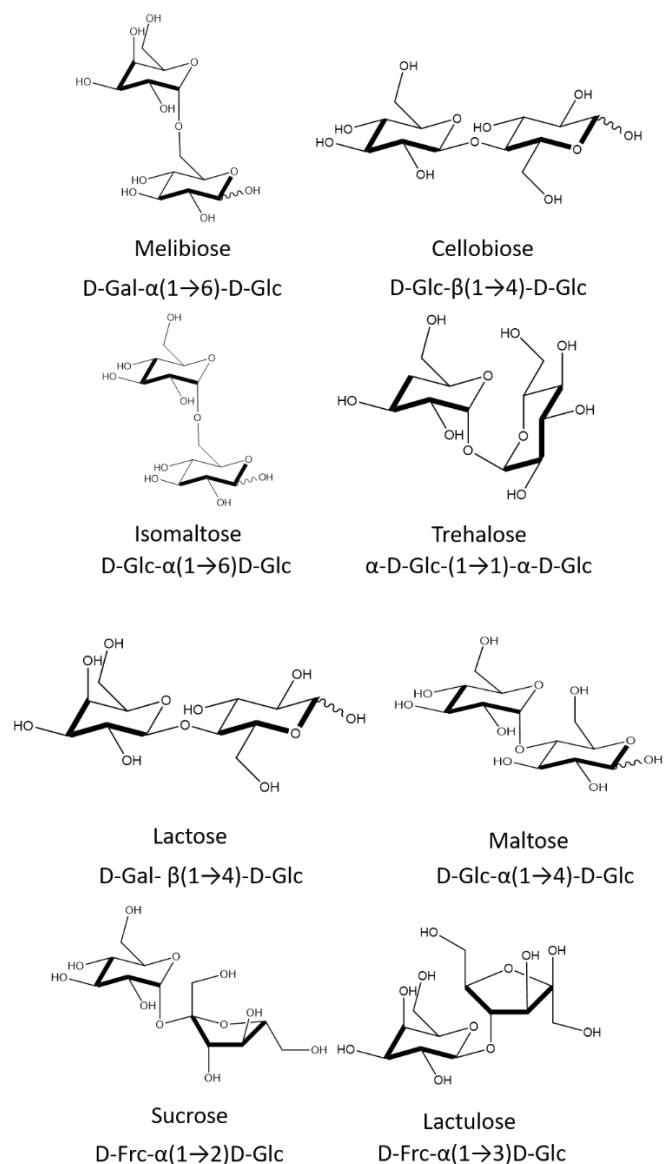


Figure 1. Structures of the isobaric disaccharides examined in this study.

The eight disaccharide analytes tested in this study are depicted in Figure 1. Maltose, trehalose, isomaltose, and cellobiose are all glucopyranosyl-glucose isomers. The remaining disaccharides included in the study contained glucose, galactose, and fructose as monomeric units. One pair of anomers, maltose and cellobiose, was included with the purpose of evaluating the utility of the studied shift reagents for distinguishing closely related stereoisomers.

Initial TWIM experiments without the addition of shift reagents showed that none of these disaccharides could be separated as their [M-H]⁻ ions, as seen in Figure 2. This was in agreement with previous studies, including one by Li *et al.*, which demonstrated that the use of ion adduction or clustering was required to separate disaccharide-derived monosaccharide-glycolaldehyde isomers using a TWIM-based approach.⁴⁹ As seen in Figure 2, all of the ATDs overlapped nearly completely, with none of them being baseline resolved. The ^{TWIM}CCS_{N₂} values for the [M-H]⁻ ions of the eight disaccharide standards are recorded in Table S-1. These ^{TWIM}CCS_{N₂} values varied from 159.6 for maltose to 163.9 for trehalose. This is a relative difference of 2.6% for the highest and lowest CCS analytes. When an established noncovalent shift reagent such as sodium, potassium, or chloride was added, a modest separation for certain pairs was observed, as shown in Figure S-1.³³ For example, sucrose and maltose were partially resolved ($R_{pp} = 1.18 \left(\frac{t_{dB} - t_{dA}}{\Delta t_{dB} + \Delta t_{dA}} \right) = 0.84$) as their potassium adducts. It was noted, however, that improvements in the separation were still needed to resolve other disaccharides, which is of particular importance in more complex mixtures where various species could co-exist.

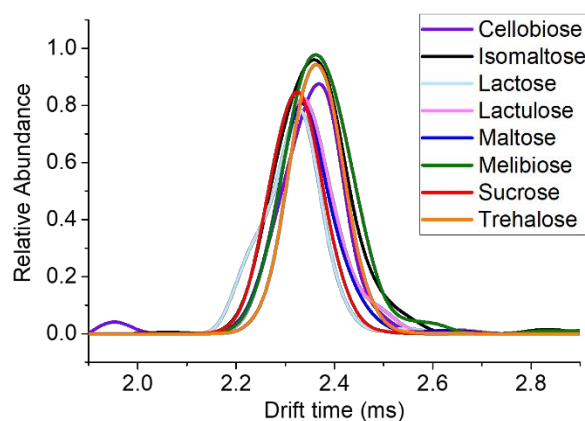


Figure 2. Overlaid arrival time distributions for the [M-H]⁻ ion of each of the eight disaccharide analytes studied. No shift reagents were used in these experiments, which were conducted by direct infusion on a Synapt G2 TWIM-MS system in negative mode with nitrogen as the buffer gas. The wave height and wave velocity were 40 V and 500 m s⁻¹, respectively.

ARTICLE

Journal Name

1
2
3
4
5
6
7
8
9
10
11
12
13
14
15
16
17
18
19
20
21
22
23
24
25
26
27
28
29
30
31
32
33
34
35
36
37
38
39
40
41
42
43
44
45
46
47
48
49
50
51
52
53
54
55
56
57
58
59
60

To this end, ten different α -amino or α -hydroxy acids (L-malic acid, NMDA, tyrosine, lactic acid, 2-hydroxyhexanoic acid, tartaric acid, arginine, N-methyl-L-glutamic acid, N-methyl-DL-aspartic acid, and citric acid) were evaluated for their potential as non-covalent IM shift reagents. These candidates were selected based on previous reports on some amino acids showing promise for monosaccharide separations.³⁹ Of the ten candidates tested, citrate was the only shift reagent considered that showed no detectable binding to any of the disaccharides investigated in this study under the studied conditions.

From these screening experiments, L-malic acid in negative ion mode and NMDA in positive ion mode were identified as the most promising shift reagents, as they showed the highest average resolution values for each possible pair of the eight disaccharides. These reagents were compared to the more established shift reagents included in Figure S-1 by assessing the resolution values as a boxplot, shown in Figure S-2. The median resolution values for the L-malic acid and NMDA complexes significantly exceeded those of chloride. While they appeared to have a higher median resolution than the sodium and potassium complexes as well, this was not a significant difference due to the high variability in resolution values. The ATD for the complexes of L-malic acid and NMDA with each of the disaccharides are shown in Figure 3. Most of the complexes showed a single peak in the ATD, implying either a single major structure or multiple structures that are too close in CCS to be resolved. However, two major peaks were observed for the lactulose/L-malic acid complex, most likely due to the shift reagent binding to different sites on lactulose. Both L-malic acid and NMDA allowed for the differentiation of most, but not all, of the disaccharide standard complexes. For example, L-malic acid showed good separation for sucrose and melibiose but less separation of cellobiose and lactulose, whereas NMDA showed good separation for cellobiose and lactulose with less separation for trehalose and cellobiose. Separations were evaluated based upon the 95% confidence interval for the CCS. Certain disaccharides were separated very well with both shift reagents, such as sucrose and cellobiose; others were more difficult to separate, such as melibiose and isomaltose. TWIM resolution for the separation of the disaccharide adducts ranged from 0.03-1.2 for NMDA and 0-1.2 for L-malic acid, as shown in Table S-2.

L-malic acid and NMDA noncovalent complexes with all disaccharide standards were also characterized by MS/MS experiments at low collision energies. Example MS/MS results

for the NMDA and L-malic acid complexes of lactose in positive and negative ion modes, respectively, are shown in Figure S-3. Due to the lower polarity of the sugar analytes relative to the shift reagents, the major product ion for each of the complexes was the ionized shift reagent itself: $[\text{NMDA}+\text{H}]^+$ in positive ion mode, and $[\text{malic acid}-\text{H}]^-$ in negative mode. Tandem MS was further used to characterize the relative binding strength of the noncovalent complexes of lactose with each of the ten shift reagents used in this study that showed detectable levels of binding. Each of these lactose complexes was fragmented at various collision energies, and the area of the precursor ion relative to the total ion area was calculated, as shown in Figure S-4. Based upon the inflection point of fitted sigmoidal curves, the strength of the binding was ranked. L-malic acid, NMDA, and tartaric acid were the weakest binding shift reagents, as $\geq 25\%$ fragmentation occurred before any collision energy was applied. The remaining complexes could be ranked from weakest to strongest binding as follows: N-methyl-DL-aspartic acid < N-methyl-L-glutamic acid < L-glutamic acid < lactic acid < 2-hydroxyhexanoic acid < tyrosine < arginine.

The noncovalent interactions between these two model shift reagents and the analytes were further characterized using molecular simulations. As an example, the lactose/L-malic acid and melibiose/NMDA complexes are shown in Figure S-5. Generally, hydrogen bonding between a hydroxyl group on the disaccharide and the charged group of the shift reagent was suggested by these calculations. Additional hydrogen bonds between hydroxyl groups on the shift reagent and disaccharide were also implied for many of these complexes. In the examples shown, two hydrogen bonds between the L-malic acid carboxylic group with two separate hydroxyl groups on the lactose, as well as an intramolecular hydrogen bond on the lactose were suggested. For the melibiose/NMDA complex, hydrogen bonds between the charged amine group on NMDA as well as the uncharged carboxylic acid group and two separate hydroxyl groups on the melibiose were involved, as well as one intramolecular hydrogen bond on the NMDA ion, and two on the melibiose molecule.

ATDs for the remaining eight shift reagents that showed binding to disaccharides, albeit with lower IM resolution are given in Figure S-6. Although there was certain degree of separation for a small number of the disaccharide pairs, there was also a significant degree of overlap for many of the complexes, so they were not pursued in further experiments.



Analyst

ARTICLE

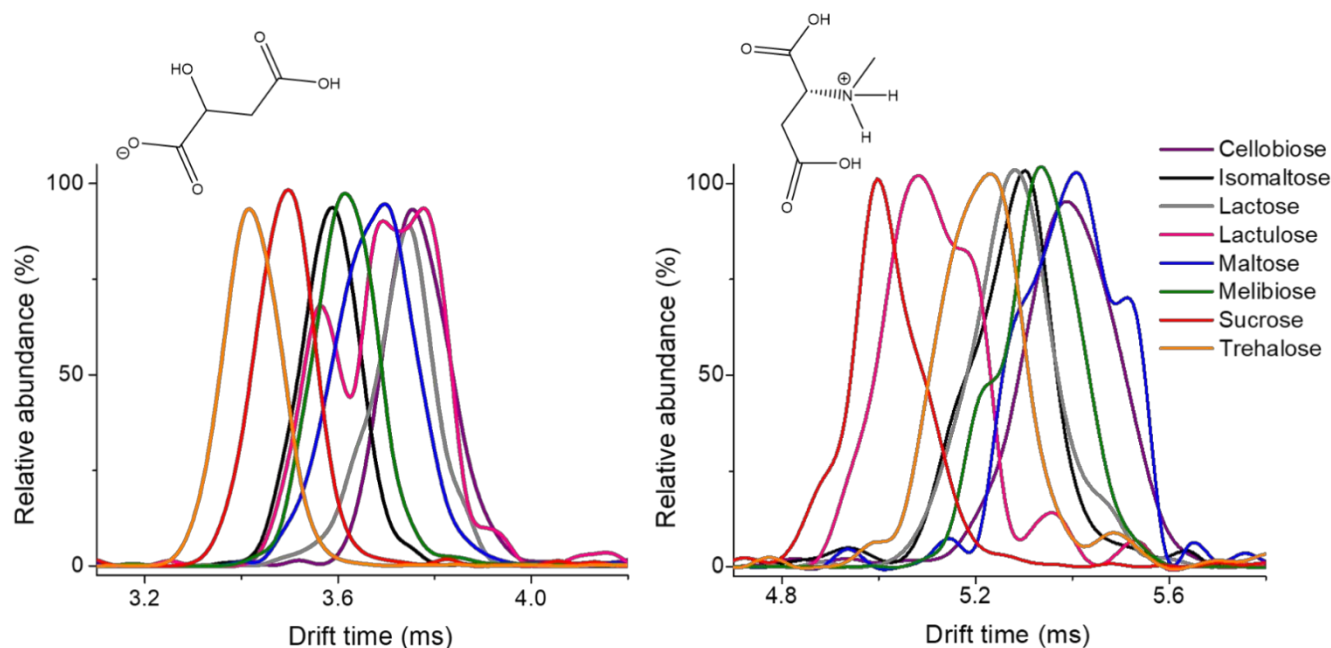


Figure 3. Overlaid arrival time distributions obtained with the Synapt G2 TWIM-MS platform for disaccharide noncovalent complexes with L-malic acid in negative ion mode (left) and N-methyl-D-aspartic acid in positive ion mode (right). The species observed are the $[M+L-H]^-$ ions (m/z 475.13) in negative ion mode and $[M+NMDA+H]^+$ ions (m/z 490.18) in positive ion mode, with M representing the neutral disaccharide and L representing neutral L-malic acid, and NMDA representing neutral N-methyl-D-aspartic acid. The wave height and wave velocity were 40 V and 500 m s^{-1} , respectively. B-spline connection was used to display these data, which smooths the peaks and may result in certain peaks appearing to be less than 100% in relative abundance.

DTIM-MS experiments were conducted to investigate whether alternative instrumentation could better resolve some of the complexes of the analyte pairs not resolved in TWIM-MS experiments. Experiments were carried out at higher overall concentrations to compensate for the lower duty cycle of the DTIM-MS instrument.⁴⁸ Overall, DTIM-MS yielded higher resolution than TWIMS (Table S-2), as seen in the arrival time distributions for L-malic acid complexes shown in Figure 4. This effect is mainly due to the higher pressure in the DTIM cell, which results in a higher number of collisions with the buffer gas. Instrumental IM resolving power ($R_p = \frac{t_d}{\Delta t_d}$) for the eight L-malic acid adducts studied improved from an average of 23 ± 5 for TWIM to 89 ± 23 for DTIM. This gain in resolving power, led to improvements in the resolution of the isobaric disaccharide analytes. While a mixture of cellobiose, melibiose, and trehalose complexes with L-malic acid appeared as two unresolved features in the ATD when using TWIM, the DTIM method was able to fully resolve one of these isomeric complexes and partially resolve the other two. This qualitatively demonstrates

the advantage of using DTIM, which was quantitatively shown in Table S-2.

Analogous to the improvements in resolution seen for L-malic acid disaccharide complexes in Figure 4 and Table S-2, DTIM also improved the resolution of NMDA complexes of cellobiose, lactose, and lactulose, as shown in Figure S-7 and in Table S-2. On average, the resolving power for the eight NMDA complexes improved from 26 ± 2 for TWIM to 107 ± 43 for DTIM. The average resolution increased from 0.49 to 1.87 in negative ion mode and from 0.48 to 2.2 in positive ion mode when comparing TWIM to DTIM (Table S-2). These results showcase the advantages of DTIM in terms of resolution, but have to be weighed against losses in sensitivity that accompany atmospheric pressure IM drift cells, mainly due to ion losses at the atmospheric pressure interface and low ion gating duty cycle.⁴⁸ The latter, however, can be offset by introducing multiplexing schemes based on Hadamard or Fourier approaches.⁵⁰⁻⁵² Cyclic TWIM-MS approaches could also be leveraged to enhance performance in combination with the new shift reagents presented here, with minimal impact on sensitivity.^{38, 53}

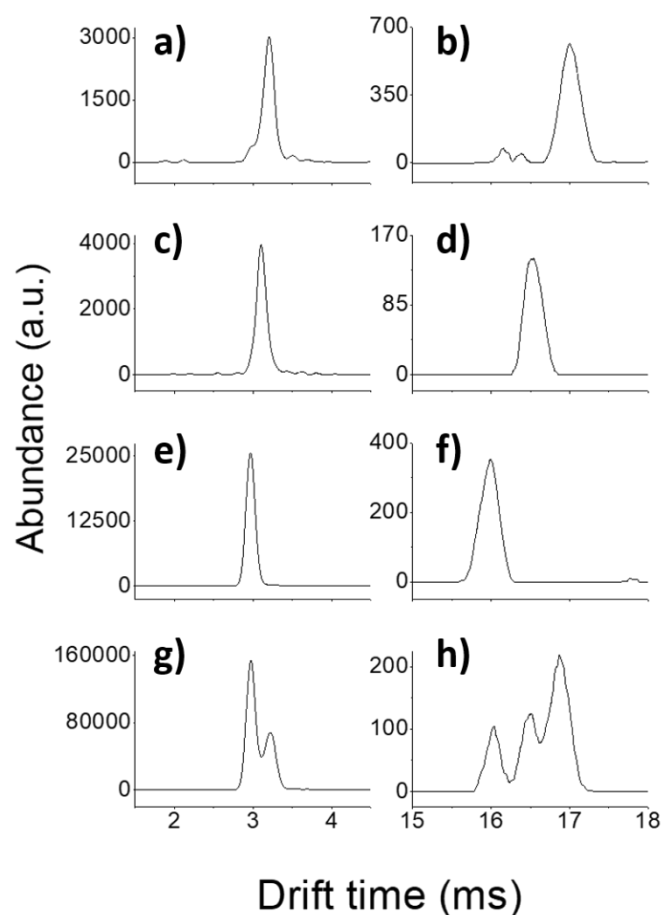


Figure 4. Comparison of arrival time distributions observed in negative ion mode Synapt G2 TWIM-MS (left column) and EXCELLIMS DTIM-Orbitrap MS (right column) experiments for selected disaccharide L-malic acid complexes. a) and b) represent the cellobiose complex, c) and d) represent that of melibiose, e) and f) represent the trehalose complex, and g) and h) represent a mixture of these three disaccharides as their L-malic acid complexes. Nitrogen was used as the buffer gas in all cases. For Synapt G2 experiments, the wave height and wave velocity were 40 V and 500 m s^{-1} , respectively. For the drift tube-Orbitrap experiment, the electric field was 765 V cm^{-1} . DTIM data was smoothed with a first order Savitzky-Golay polynomial function using a window width of 12.

While both L-malic acid and NMDA demonstrated an advantage over more traditional noncovalent shift reagents such as group I metal cations, neither achieved full IM separation of all possible combinations of the eight analytes

with either IM method tested in this study. For example, cellobiose/lactulose and cellobiose/lactose were separated as their NMDA complexes but not as their L-malic acid complexes. In contrast, lactose/isomaltose and maltose/cellobiose were differentiated as their L-malic acid complexes but not as their NMDA complexes.

To further examine alternative approaches for distinguishing between these analytes, collision cross section (CCS) values for each of the L-malic acid and NMDA complexes were calculated from their TWIM arrival times, following methods reported by Forsythe *et al.*²⁹ CCS values were also directly calculated from DTIM measurements (Tables S-3 and S-4). $^{TWIM}CCS_{N_2}$ calibration curves for polymalic acid and polyalanine in negative ion mode are provided in Figure S-8, showing excellent linearity. Overall, TWIM results showed that $^{TWIM}CCS_{N_2}$ values for L-malic acid complexes ranged from 194.2 \AA^2 for sucrose to 201.8 \AA^2 for lactulose, while the NMDA complexes ranged from 198.3 \AA^2 for sucrose to 206.9 \AA^2 for cellobiose. Negative ion mode $^{TWIM}CCS_{N_2}$ values calculated by calibration with polymalic acid and polyalanine were not significantly different at the 95% confidence level for any of the L-malic acid complexes ($n=4$). NMDA complexes were only calibrated with polyalanine, as polymalic acid does not ionize well in positive mode. Due to differences in the temperature and pressure operating ranges of the DTIM and TWIM IM-MS platforms utilized in this study, $^{TWIM}CCS_{N_2}$ and $^{DTIM}CCS_{N_2}$ values could not be directly compared and were not expected to match. $^{DTIM}CCS_{N_2}$ values were significantly larger than $^{TWIM}CCS_{N_2}$ values, with the L-malic acid complexes ranging from 298.3 \AA^2 for trehalose to 320.7 \AA^2 for lactulose, and the NMDA complexes ranging from 312.8 \AA^2 for sucrose to 326.8 \AA^2 for lactose.

We hypothesized that L-malic acid and NMDA CCS values could be used in a complementary manner to distinguish every analyte within this study. The use of a combination of IM-derived CCS values for several shift reagent complexes has been reported in the past.^{33, 39, 42} Gaye *et al.*, for example, showed that the combination of $[M+L\text{-serine}+H]^+$, $[M+L\text{-phenylalanine-glycine}+H]^+$, and $[Mn^{II} + (L\text{-phenylalanine-glycine-H})+M]^+$ resulted in the "virtual separation" of 16 monosaccharide isobars when their CCS values were represented in 3D space.³⁹ Accordingly, $^{TWIM}CCS_{N_2}$ values for NMDA and L-malic acid disaccharide complexes were combined, which allowed for all of the eight analytes to be fully distinguished from one another at the 95% confidence level (Figure 5).



Analyst

ARTICLE

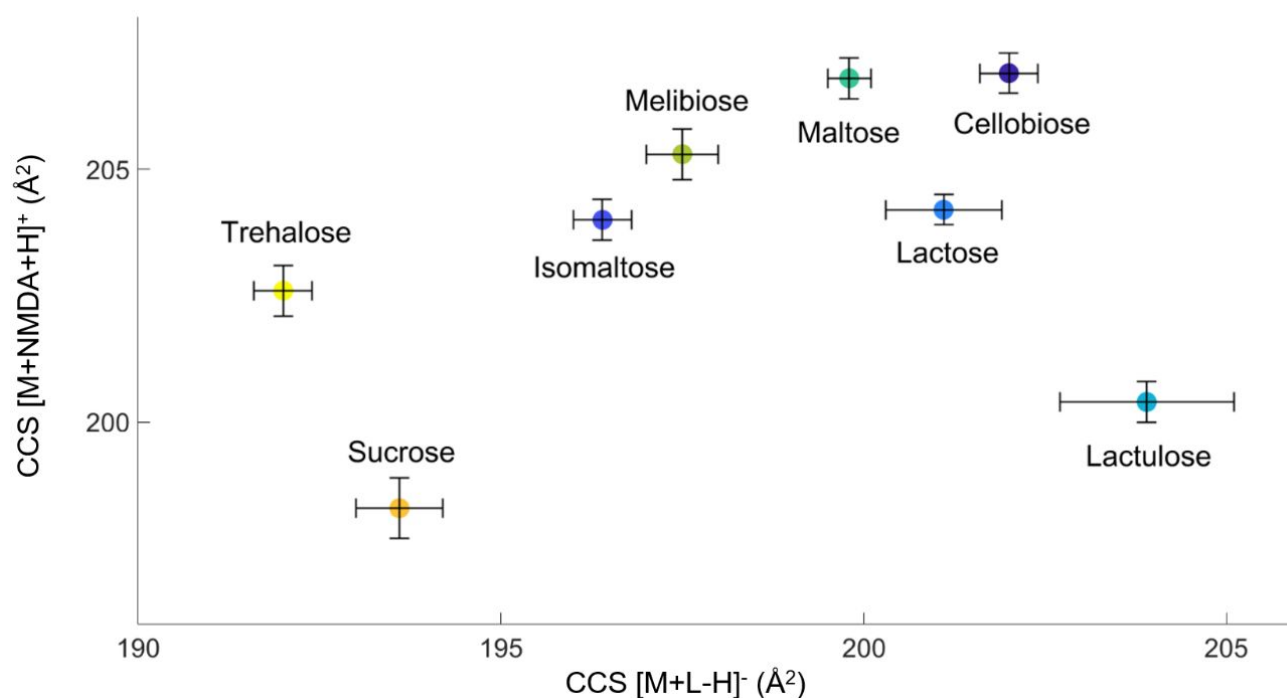


Figure 5. Ion-neutral $^{TWIM}CCS_{N_2}$ values for the dominant feature in the arrival time distribution for each of the various tested disaccharides as their $[M+NMDA+H]^+$ N-methyl-D-aspartic complexes versus their corresponding $^{TWIM}CCS_{N_2}$ for the $[M+L-H]^-$ L-malic acid complexes. Error bars represent the 95% confidence interval determined by four trials per complex. The colormap corresponds to the L-malic acid complex CCS. All CCS values are the average of four measurements with polyalanine used for calibration.

Conclusions

Noncovalent α -hydroxy and amino acid shift reagents, specifically L-malic acid and NMDA, showed promise in separating disaccharide isomers by IM-MS. By TWIM, eight disaccharides could be distinguished at 95% confidence by determining the CCS of their L-malic acid adducts in negative ion mode and their NMDA adducts in positive ion mode. Using DTIM, the resolution of these separations was further improved. Additional high-resolution techniques, such as cyclic IM could be used to apply this method to more complex mixtures of disaccharides. The proposed methodology could be combined with other shift reagents or additional separation techniques (*e.g.* LC) to characterize complex mixtures of carbohydrates, such as those generated by the model prebiotic reactions that mimic early Earth conditions or biological extracts. We expect that quantitation would be possible if adequate chemical standards are available for appropriate calibration without significant interferences or matrix effects.

Conflicts of interest

There are no conflicts to declare.

Acknowledgements

This work was jointly supported by NSF and the NASA Astrobiology Program, under the NSF Center for Chemical Evolution, CHE-1504217. We would also like to acknowledge Prof. Jesse McDaniel for help with MD calculations and Prof. Jay Forsythe at the College of Charleston for his insightful comments and suggestions for improving early drafts of this manuscript.

References

- (1) Gamblin, D. P.; Scanlan, E. M.; Davis, B. G., *Chem. Rev.* **2009**, *109* (1), 131-163.
- (2) Krogh, A.; Lindhard, J., *Biochem. J.* **1920**, *14* (3-4), 290-363.
- (3) Abbott, D. W.; Ficko-Blean, E.; van Bueren, A. L.; Rogowski, A.; Cartmell, A.; Coutinho, P. M.; Henrissat, B.; Gilbert, H. J.; Boraston, A. B., *Biochemistry* **2009**, *48* (43), 10395-10404.

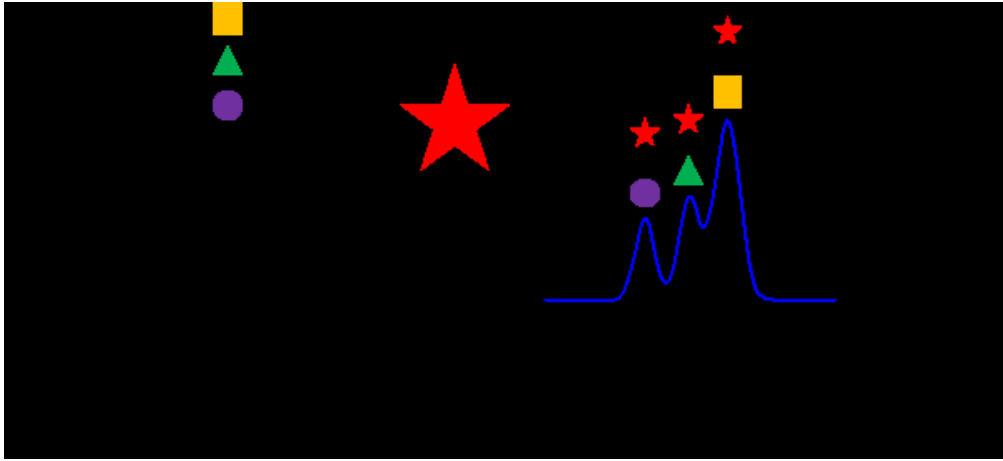
- (4) de la Fuente, J. M.; Penadés, S., *Glycoconjugate J.* **2004**, *21* (3), 149-163.
- (5) Dennis, J. W.; Granovsky, M.; Warren, C. E., *Bioessays* **1999**, *21* (5), 412-21.
- (6) Gabius, H.-J.; Siebert, H.-C.; André, S.; Jiménez-Barbero, J.; Rüdiger, H., *ChemBioChem* **2004**, *5* (6), 740-764.
- (7) Tolstoguzov, V., *Carbohydr. Polym.* **2003**, *54* (3), 371-380.
- (8) Stern, R.; Jedrzejak, M. J., *Chem. Rev.* **2008**, *108* (12), 5061-5085.
- (9) Li, Z.; Li, L.; McKenna, K. R.; Schmidt, M.; Pollet, P.; Gelbaum, L.; Fernández, F. M.; Krishnamurthy, R.; Liotta, C. L., *Origins of Life and Evolution of Biospheres* **2019**, *49* (4), 225-240.
- (10) Schramm, G.; Grötsch, H.; Pollmann, W., *Angewandte Chemie International Edition in English* **1962**, *1* (1), 1-7.
- (11) Dwek, R. A., *Chem. Rev.* **1996**, *96* (2), 683-720.
- (12) Dell, A.; Morris, H. R.; Easton, R. L.; Panico, M.; Patankar, M.; Oehninger, S.; Koistinen, R.; Koistinen, H.; Seppala, M.; Clark, G. F., *J. Biol. Chem.* **1995**, *270* (41), 24116-24126.
- (13) Mottram, D. S.; Wedzicha, B. L.; Dodson, A. T., *Nature* **2002**, *419* (6906), 448-449.
- (14) Fry, S. C., *Planta* **1983**, *157* (2), 111-123.
- (15) Koizumi, K.; Okada, Y.; Fukuda, M., *Carbohydr. Res.* **1991**, *215* (1), 67-80.
- (16) Zhou, S.; Huang, Y.; Dong, X.; Peng, W.; Veillon, L.; Kitagawa, D. A. S.; Aquino, A. J. A.; Mechref, Y., *Anal. Chem.* **2017**, *89* (12), 6590-6597.
- (17) Guile, G. R.; Rudd, P. M.; Wing, D. R.; Prime, S. B.; Dwek, R. A., *Anal. Biochem.* **1996**, *240* (2), 210-26.
- (18) Azenha, C. S.; Coimbra, M. A.; Moreira, A. S.; Domingues, P.; Domingues, M. R., *J. Mass Spectrom.* **2013**, *48* (5), 548-52.
- (19) Kuki, Á.; Szabó, K. E.; Nagy, L.; Zsuga, M.; Kéki, S., *J. Mass Spectrom.* **2013**, *48* (12), 1276-1280.
- (20) Baker, E. S.; Burnum-Johnson, K. E.; Jacobs, J. M.; Diamond, D. L.; Brown, R. N.; Ibrahim, Y. M.; Orton, D. J.; Piehowski, P. D.; Purdy, D. E.; Moore, R. J.; Danielson, W. F.; Monroe, M. E.; Crowell, K. L.; Slysz, G. W.; Gritsenko, M. A.; Sandoval, J. D.; LaMarche, B. L.; Matzke, M. M.; Webb-Robertson, B.-J. M.; Simons, B. C.; McMahon, B. J.; Bhattacharya, R.; Perkins, J. D.; Carithers, R. L.; Strom, S.; Self, S. G.; Katze, M. G.; Anderson, G. A.; Smith, R. D., *Molecular & Cellular Proteomics* **2014**, *13* (4), 1119-1127.
- (21) Hofmann, J.; Hahm, H. S.; Seeberger, P. H.; Pagel, K., *Nature* **2015**, *526* (7572), 241-4.
- (22) Clowers, B. H.; Dwivedi, P.; Steiner, W. E.; Hill, H. H.; Bendiak, B., *J. Am. Soc. Mass. Spectrom.* **2005**, *16* (5), 660-669.
- (23) Kyle, J. E.; Zhang, X.; Weitz, K. K.; Monroe, M. E.; Ibrahim, Y. M.; Moore, R. J.; Cha, J.; Sun, X.; Lovelace, E. S.; Wagoner, J.; Polyak, S. J.; Metz, T. O.; Dey, S. K.; Smith, R. D.; Burnum-Johnson, K. E.; Baker, E. S., *Analyst* **2016**, *141* (5), 1649-1659.
- (24) Smith, D. P.; Giles, K.; Bateman, R. H.; Radford, S. E.; Ashcroft, A. E., *J. Am. Soc. Mass. Spectrom.* **2007**, *18* (12), 2180-2190.
- (25) Cohen, M. J.; Karasek, F. W., *J. Chromatogr. Sci.* **1970**, *8* (6), 330-337.
- (26) Giles, K.; Pringle, S. D.; Worthington, K. R.; Little, D.; Wildgoose, J. L.; Bateman, R. H., *Rapid Commun. Mass Spectrom.* **2004**, *18* (20), 2401-2414.
- (27) Mason, E. A.; McDaniel, E. W., *Transport Properties of Ions in Gases* **1988**.
- (28) Smith, D. P.; Knapman, T. W.; Campuzano, I.; Malham, R. W.; Berryman, J. T.; Radford, S. E.; Ashcroft, A. E., *Eur. J. Mass Spectrom.* **2009**, *15* (2), 113-130.
- (29) Forsythe, J. G.; Petrov, A. S.; Walker, C. A.; Allen, S. J.; Pellissier, J. S.; Bush, M. F.; Hud, N. V.; Fernandez, F. M., *Analyst* **2015**, *140* (20), 6853-61.
- (30) Gelb, A. S.; Jarratt, R. E.; Huang, Y.; Dodds, E. D., *Anal. Chem.* **2014**, *86* (22), 11396-11402.
- (31) Williams, J. P.; Grabenauer, M.; Holland, R. J.; Carpenter, C. J.; Wormald, M. R.; Giles, K.; Harvey, D. J.; Bateman, R. H.; Scrivens, J. H.; Bowers, M. T., *Int. J. Mass Spectrom.* **2010**, *298* (1), 119-127.
- (32) Morrison, K. A.; Bendiak, B. K.; Clowers, B. H., *J. Am. Soc. Mass. Spectrom.* **2017**, *28* (4), 664-677.
- (33) Huang, Y.; Dodds, E. D., *Anal. Chem.* **2013**, *85* (20), 9728-9735.
- (34) Huang, Y.; Dodds, E. D., *Anal. Chem.* **2015**, *87* (11), 5664-5668.
- (35) Li, H.; Bendiak, B.; Siems, W. F.; Gang, D. R.; Hill, H. H., *Rapid communications in mass spectrometry : RCM* **2013**, *27* (23), 2699-2709.
- (36) Yang, H.; Shi, L.; Zhuang, X.; Su, R.; Wan, D.; Song, F.; Li, J.; Liu, S., *Sci. Rep.* **2016**, *6*.
- (37) Li, L.; McKenna, K. R.; Li, Z.; Yadav, M.; Krishnamurthy, R.; Liotta, C. L.; Fernandez, F. M., *Analyst* **2018**, *143* (4), 949-955.
- (38) McKenna, K. R.; Li, L.; Baker, A. G.; Ujma, J.; Krishnamurthy, R.; Liotta, C. L.; Fernández, F. M., *Analyst* **2019**, *144* (24), 7220-7226.
- (39) Gaye, M. M.; Nagy, G.; Clemmer, D. E.; Pohl, N. L. B., *Anal. Chem.* **2016**, *88* (4), 2335-2344.
- (40) Chaffey, N., *Ann Bot* **2014**, *113* (7), vii-vii.
- (41) Bush, M. F.; Campuzano, I. D. G.; Robinson, C. V., *Anal. Chem.* **2012**, *84* (16), 7124-7130.
- (42) Zheng, X.; Zhang, X.; Schocker, N. S.; Renslow, R. S.; Orton, D. J.; Khamsi, J.; Ashmus, R. A.; Almeida, I. C.; Tang, K.; Costello, C. E.; Smith, R. D.; Michael, K.; Baker, E. S., *Anal. Bioanal. Chem.* **2017**, *409* (2), 467-476.
- (43) Pence, H. E.; Williams, A., *J. Chem. Educ.* **2010**, *87* (11), 1123-1124.
- (44) Hanwell, M. D.; Curtis, D. E.; Lonie, D. C.; Vandermeersch, T.; Zurek, E.; Hutchison, G. R., *J. Cheminform* **2012**, *4* (1), 17-17.
- (45) Valiev, M.; Bylaska, E. J.; Govind, N.; Kowalski, K.; Straatsma, T. P.; Van Dam, H. J. J.; Wang, D.; Nieplocha, J.; Apra, E.; Windus, T. L.; de Jong, W. A., *Comput. Phys. Commun.* **2010**, *181* (9), 1477-1489.
- (46) Becke, A. D., *The Journal of Chemical Physics* **1993**, *98* (7), 5648-5652.
- (47) Francl, M. M.; Pietro, W. J.; Hehre, W. J.; Binkley, J. S.; Gordon, M. S.; DeFrees, D. J.; Pople, J. A., *The Journal of Chemical Physics* **1982**, *77* (7), 3654-3665.
- (48) Keelor, J. D.; Zambrzycki, S.; Li, A.; Clowers, B. H.; Fernández, F. M., *Anal. Chem.* **2017**, *89* (21), 11301-11309.
- (49) Li, H.; Bendiak, B.; Siems, W. F.; Gang, D. R.; Hill Jr, H. H., *Rapid Commun. Mass Spectrom.* **2013**, *27* (23), 2699-2709.
- (50) Clowers, B. H.; Siems, W. F.; Hill, H. H.; Massick, S. M., *Anal. Chem.* **2006**, *78* (1), 44-51.
- (51) Prost, S. A.; Crowell, K. L.; Baker, E. S.; Ibrahim, Y. M.; Clowers, B. H.; Monroe, M. E.; Anderson, G. A.; Smith, R. D.; Payne, S. H., *J. Am. Soc. Mass. Spectrom.* **2014**, *25* (12), 2020-2027.
- (52) Morrison, K. A.; Siems, W. F.; Clowers, B. H., *Anal. Chem.* **2016**, *88* (6), 3121-3129.
- (53) Ujma, J.; Ropartz, D.; Giles, K.; Richardson, K.; Langridge, D.; Wildgoose, J.; Green, M.; Pringle, S., *J. Am. Soc. Mass. Spectrom.* **2019**, *30* (6), 1028-1037.



1
2
3
4 **Analyst**
5
6

7 ARTICLE
8
9
10
11
12
13
14
15
16
17
18
19
20
21
22
23
24
25
26
27
28
29
30
31
32
33
34
35
36
37
38
39
40
41
42
43
44
45
46
47
48
49
50
51
52
53
54
55
56
57
58
59
60

1
2
3
4
5
6
7
8
9
10
11
12
13
14
15
16
17
18
19
20
21
22
23
24
25
26
27
28
29
30
31
32
33
34
35
36
37
38
39
40
41
42
43
44
45
46
47
48
49
50
51
52
53
54
55
56
57
58
59
60



101x46mm (150 x 150 DPI)